Development 138, 149-158 (2011) doi:10.1242/dev.056309

Megalin-dependent Yellow endocytosis restricts melanization in the *Drosophila* cuticle

Falko Riedel, Daniela Vorkel and Suzanne Eaton*

SUMMARY

The cuticular exoskeleton of arthropods is a composite material comprising well-separated layers that differ in function and molecular constituents. Epidermal cells secrete these layers sequentially, synthesizing components of distal cuticle layers before proximal ones. Could the order of synthesis and secretion be sufficient to account for the precision with which cuticle components localize to specific layers? We addressed this question by studying the spatial restriction of melanization in the *Drosophila* wing. Melanin formation is confined to a narrow layer within the distal procuticle. Surprisingly, this tight localization depends on the multi-ligand endocytic receptor Megalin (Mgl). Mgl acts, in part, by promoting endocytic clearance of Yellow. Yellow is required for black melanin formation, and its synthesis begins as cuticle is secreted. Near the end of cuticle secretion, its levels drop precipitously by a mechanism that depends on Mgl and Rab5-dependent endocytosis. In the absence of Mgl, Yellow protein persists at higher levels and melanin granules form ectopically in more proximal layers of the procuticle. We propose that the tight localization of the melanin synthesis machinery to the distal procuticle depends not only on the timing of its synthesis and secretion, but also on the rapid clearance of these components before synthesis of subsequent cuticle layers.

KEY WORDS: Cuticle, *Drosophila*, Megalin, Yellow

INTRODUCTION

Cuticle is a fascinating and highly versatile composite material that constitutes the exoskeleton of arthropods. It consists of functionally distinct layers. The outermost layer consists of a lipid-rich waterproofing envelope and an epicuticle containing highly crosslinked proteins. Beneath this lies a mechanically resilient procuticle consisting of chitin embedded in a protein matrix (Locke, 2001; Moussian, 2010). Procuticle can be separated into ultrastructurally distinct layers that differ in chitin organization, protein composition and pigmentation (Fristrom et al., 1986; Kayser-Wegmann, 1976). The properties of the different cuticle layers also vary widely in different body regions, producing cuticles with specialized mechanical properties (Vincent and Wegst, 2004) and a stunning variety of pigmentation patterns.

The organization of cuticle in distinct layers reflects the ordered synthesis and secretion of different cuticular components by ectodermal epithelial cells (Doctor et al., 1985; Fristrom et al., 1986; Locke, 2001; Mitchell et al., 1983; Moussian, 2010). However, the different layers also continue to develop and change their appearance after secretion as the cuticle matures (Moussian et al., 2006). After cuticle secretion, ectodermal cells release a variety of catecholamine compounds (dopamine, N-β-alanyl dopamine and N-acetyl dopamine), which are derived from circulating tyrosine (Andersen, 2009; Hopkins and Kramer, 1992; Walter et al., 1991; Wright, 1987). Cuticular phenoloxidases oxidize these catecholemines to quinones, which are used to produce melanin for pigmentation and to crosslink cuticle proteins, a process called sclerotization (see Fig. 1).

Max Planck Institute of Molecular Cell Biology and Genetics, Pfotenhauerstrasse-108, Dresden 01307, Germany.

*Author for correspondence (eaton@mpi-cbg.de)

Accepted 19 October 2010

Melanins are an ancient and heterogeneous family of polymeric pigments used throughout the animal kingdom (Sugumaran, 2002). The black eumelanins are produced as quinones derived from dopamine and undergo a series of cyclization and oxidation reactions and then polymerize. This process requires the royal jelly family protein Yellow, which is deposited into the cuticle before pigmentation (Kornezos and Chia, 1992; Walter et al., 1991; Wittkopp et al., 2002) (see Fig. 1). In *yellow* mutant flies, production of black melanin is blocked and sulfur-containing pheomelanins accumulate (Latocha et al., 2000). How Yellow guides these reactions is unknown, although two other family members, Yellow-f1 and Yellow-f2, have dopachrome conversion activity (Han et al., 2002). Regulation of pigment formation is spatially precise. It occurs in specific patterns (Wittkopp and Beldade, 2009; Wittkopp et al., 2002) and localizes to specific cuticle layers (Kayser-Wegmann, 1976). How do ectodermal epithelial cells achieve this? Could such exquisite organization be produced simply by the order and pattern in which pigmentation components are secreted?

Here, we describe a novel function for Megalin (Mgl)-dependent endocytosis in structuring the *Drosophila* cuticle. Mgl is a large low-density lipoprotein receptor-related protein (LRP) that is broadly expressed in epithelial tissues and mediates endocytosis of a wide range of ligands from the apical surface (Christensen and Willnow, 1999; Moestrup and Verroust, 2001). We find that Mgl-dependent endocytosis of Yellow restricts its localization, thereby limiting pigment formation to the distal procuticle.

MATERIALS AND METHODS

Dopamine determinations

The wings of five pupae aged for 63 hours after puparium formation (apf) at 29°C were dissected in PBS, collected in 50 μl 1 N HCl, frozen in liquid nitrogen and stored at –80°C. Samples were thawed at room temperature and homogenized with Biovortexer (Biospec products). The dopamine concentration of 40 μl of this homogenate was determined with a dopamine ELISA according to the instructions of the manufacturer (Labor Diagnostika Nord).

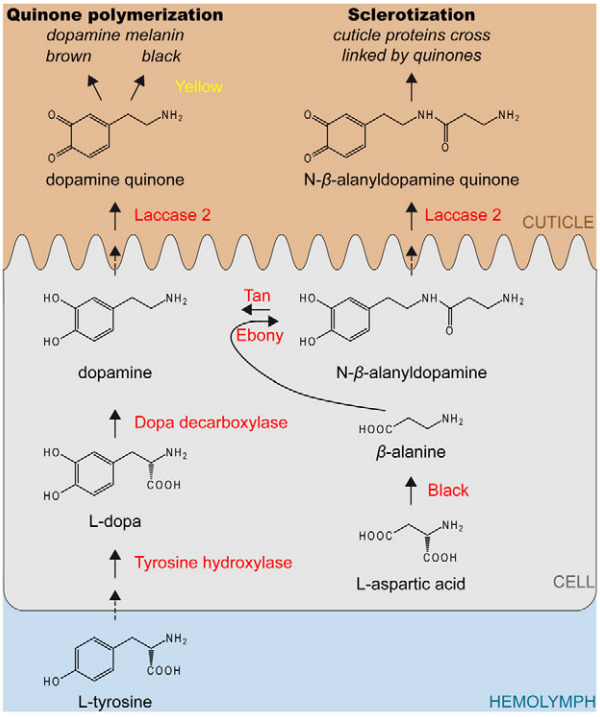

Fig. 1. Catecholamine pathway leading to sclerotization and pigmentation of the cuticle of *Drosophila melanogaster*. Shown is an epithelial cell (grey), which contacts hemolymph (blue) basally and secretes cuticle (brown) apically. Dashed arrows indicate unknown transport pathways, solid arrows denote reactions catalysed by the indicated enzymes (red) or mediated by the indicated catecholamine quinones themselves. Tyrosine taken up from the hemolymph is converted in epithelial cells to L-dopa by tyrosine hydroxylase and then to dopamine by dopa decarboxylase. Some dopamine is released into the cuticle, where it is oxidized by Laccase 2 to dopamine quinone. In the presence of Yellow, dopamine quinone polymerizes to form black melanin. Some dopamine is conjugated with β-alanine by Ebony to produce N-β-alanyl dopamine, and the reverse reaction is catalysed by Tan. Upon release of N-β-alanyl dopamine into the cuticle, it is oxidized by Laccase 2 to a quinone, which mediates cuticle protein cross-linking (sclerotization). Adapted from True et al. (True et al., 2005), modified according to Walter et al. (Walter et al.,1996) and results shown in this work.

Stocks

Deletions in the *mgl* locus were generated by imprecise excision of the EP-element GE3293 from Genexel (Hong et al., 2006), which lies in an intron of *mgl* (*CG42611*). Out of 639 excision lines screened by PCR, six lines (mgl^{168}, mgl^{269}, mgl^{285}, mgl^{406}, mgl^{608} and mgl^{793}) were found to carry a deletion that affects the predicted open reading frame of *mgl*. mgl^{793} is homozygous viable and does not affect Mgl protein levels. Animals homozygous for the other five alleles die before adulthood and rarely develop into crawling third instar larva. Mgl protein is undetectable by immunohistochemistry in wing discs from homozygous mutant third instar larvae for these five lines when compared with wild-type wing discs (not shown). Additional details can be found in Fig. S6 in the supplementary material.

The following stocks have been obtained from the Bloomington Drosophila Stock Center and are described in FlyBase: *FM7i, actGFP/C(1)DX,* y^1 f^1*, w hs-flp,* y^1 *w** v^{24} *FRT18E,* y^1 w^{1118}*; Ubi-GFP.nls FRT18E;* $Kr^{If\text{-}1}$*/CyO,* w^{1118}*; MKRS, hs-flp86E/TM6B, en-GAL4, ap-GAL4,* C765-GAL4, hh-GAL4.

The *pFRIPE-UAS-mgl-shRNA*[1], *pUhr-UAS-Rab5SN* and *UAS-yellow* stocks have been described (Khaliullina et al., 2009; Marois et al., 2006; Wittkopp et al., 2002).

The *pFRIPE-UAS-mgl shRNA*[2] stock carries a pFRiPE derivative containing nucleotides 10272-10757 of *CG42611-RA* as a repeat unit.

The *UAS-laccase 2 shRNA*, *UAS-tyrosine hydroxylase shRNA*, *UAS-mgl shRNA*[3] and *UAS-yellow shRNA* stocks carry nucleotides 1390-1750 of *CG42345-RA*, 1885-2151 of *pale-RB*, 5780-6151 of *CG42611-RA* and 1063-1312 of the *yellow-RA* transcript, respectively, as a repeat unit and were obtained from the Vienna Drosophila RNAi Center (Dietzl et al., 2007).

Unless otherwise noted, crosses were kept at 25°C for five days and then transferred to 29°C. Crosses involving *pFRIPE-UAS-mgl-shRNA* constructs were heat shocked at 37°C for 1.5 hours (to remove the intervening HcRed cassette) before transferring them to 29°C (Marois and Eaton, 2007). The induction of *mgl* RNAi in only a subset of *GAL4*-expressing cells was achieved by a heat shock at 37°C for 20 minutes only. In order to examine the pigmentation of adult wings expressing *pUhr-UAS-Rab5SN*, the HcRed cassette was removed by heat shocking at 47 hours apf (29°C). To examine Yellow distribution or in vitro melanization, these wings were heat shocked at 35 hours apf (29°C). *mgl* mutant clones were generated by heat shocking larvae four days after egg laying for 1 hour at 37°C, placing larvae at 29°C and dissecting third instar larvae three days later.

Immunohistochemistry

Larval wing discs were stained as described by Khaliullina et al. (Khaliullina et al., 2009). To stain embryos with Fasciclin III, Mgl, Crumbs or E-Cadherin, embryos were chemically fixed with 4% paraformaldehyde (PFA) according to standard methods. To stain embryos with antibodies including anti-Yellow, embryos were dechorionated, transferred to a boiling solution of 0.03% Triton X-100 and 68 mM NaCl and cooled down with an ice cold solution of 0.03% Triton X-100 and 68 mM NaCl for 1 minute. After removal of Triton X-100 and NaCl, embryos were processed as for chemical fixation. To stain sectioned pupal wings, pupae aged for the desired amount of time at 29°C were removed from the pupal case in PBS. Wings were removed, fixed in 4% PFA for 20 minutes and washed 3× in PBS for 10 minutes. Samples were incubated in PBS with 10% sucrose for 30 minutes followed by an overnight incubation in PBS with 20% sucrose at 4°C. The wings were embedded in NEG 50 frozen section medium (Thermo Scientific), frozen on dry ice and stored at –80°C. The frozen specimen was sectioned in 12 μm thick slices with an HM 560 Cryo-Star cryostat (Microm). The sections were collected on Superfrost Plus microscope slides (Menzel) and surrounded with an Immedge Hydrophobic Pen (Vector Laboratories). Immunohistochemical stainings of pupal wing sections were done using standard protocols.

The following primary antibodies have been used: rabbit anti-Yellow (1:200) (Wittkopp et al., 2002), guinea pig anti-Mgl (1:200) (Khaliullina et al., 2009), rat anti-E-Cadherin (1:100, Developmental Studies Hybridoma Bank) (Oda et al., 1994), mouse anti-Fasciclin III (1:100) (Developmental Studies Hybridoma Bank) (Patel et al., 1987), rat anti-Crumbs (1:500) (Richard et al., 2006).

The following secondary antibodies were used, each at a concentration of 1:1000: Cy3 or Cy5 conjugated donkey anti-mouse, anti-rabbit, anti-guinea pig or anti-rat IgG (Jackson ImmunoResearch), AlexaFluor 488-conjugated goat anti-rabbit IgG (Invitrogen).

Chitin was detected with a fluorescein-conjugated chitin binding probe (1:500, NEB) (Devine et al., 2005).

Images were acquired with a LSM 510 Laser Scanning Microscope (Zeiss).

Western blotting

Pupae aged for the desired amount of time were removed from the pupal case in PBS. For each genotype and timepoint, the wings of four males or females were collected in 40 μl PBS with complete protease inhibitor cocktail (Roche). The wings were homogenized with Biovortexer (Biospec products), mixed with 10 μl 5× SDS loading buffer, frozen in liquid nitrogen and stored at –20°C. Eight microlitres of the sample were analyzed by western blotting using standard procedures.

The primary antibodies used were: rabbit anti-Yellow antibody (1:1000) (Wittkopp et al., 2002), mouse anti-α-Tubulin antibody (1:3000, Sigma-Aldrich).

The following horseradish peroxidase-conjugated secondary antibodies were used: goat anti-rabbit IgG (1:5000, Santa Cruz), goat anti-mouse IgG (1:5000, Jackson ImmunoResearch).

Microscopy of adult wings

Wings of adults aged for 3 days after eclosion were collected in a 1:3 glycerol-ethanol mixture, washed in water, transferred to ethanol and mounted in Euparal (Roth). Wings were imaged with a Spot RT Slider 2.3.1 (Visitron Systems) mounted on an Axioplan 2 Imaging microscope (Carl Zeiss).

Light micrographs of living, anaesthetized adult flies were taken with a Stemi SV 11 (Carl Zeiss) equipped with a Progress C10 Plus (Jenoptik).

Electron microscopy

Pupae aged for the desired amount of time at 29°C were placed in 2.5% glutaraldehyde in PBS. The operculum was removed, the pupa cut transversally in the middle of the abdomen with scissors and incubated for 1 hour in fixative. The puparium case was cut on the dorsal side with scissors and removed completely from the animal. The pupal cuticle was removed and the wings taken off with forceps. Wings were kept overnight in fixative at 4°C and washed 3× in PBS for 15 minutes and 3× in water for 15 minutes. Tissues were postfixed in 1% OsO_4, rinsed 3× in water and dehydrated in a graded ethanol series. Pupal wings were embedded in serial steps using a mixture of EmBed-812 (Science Services) and ethanol. Sections were poststained with uranyl acetate and lead citrate.

For electron microscopy of in vitro melanized wings, pupae were aged for 59 to 60 hours at 29°C. Wings were dissected as described above for unmelanized wings except that the pupae were opened in PBS and fixed for only 30 minutes followed by three washes in PBS for 5 minutes. Melanization was induced for 1.5 hours in 5.3 mM dopamine hydrochloride in PBS. Wings were washed 3× in PBS for 5 minutes and incubated in 2.5% glutaraldehyde overnight at 4°C. The samples were further processed as described for unmelanized pupal wings except that no poststaining was applied.

For electron microscopy of adult wings, adults were collected before wing expansion on ice, submerged in ethanol and fixed for 2 hours in 2.5% glutaraldehyde in PBS. Wings were further processed as described for unmelanized pupal wings except that embedding was done with a mixture of EmBed-812 and acetone.

Ultrathin 70 nm transversal sections were prepared with an Ultracut UCT microtome (Leica Microsystems). Electron micrographs were taken with a Tecnai 12 electron microscope (Phillips).

In vitro melanization of pupal wings

We modified the method described by Walter et al. (Walter et al., 1996). Pupae incubated for 58 to 60 hours apf (29°C) were placed in PBS. Pharate adults were removed from the pupal case and the pupal cuticle was detached. The wings were inflated in water for 5 minutes. Pharate adults were fixed in 4% PFA in PBS for 30 minutes while their wings were being removed. Wings were washed 3× in PBS for 5 minutes. Melanization was induced in 5.3 mM dopamine hydrochloride in PBS for 1.5 hours at room temperature. Samples were washed 3× in PBS for 5 minutes and postfixed in 4% paraformaldehyde overnight at 4°C. Wings were dehydrated in a graded ethanol series in PBS, cleared in xylene and mounted in Canada balsam. Wings were imaged as described for adult wings.

RESULTS

Loss of Megalin alters cuticle color and mechanical resilience

To study the function of Mgl during *Drosophila* development, we first examined its tissue distribution. Mgl is expressed throughout the cuticle-secreting ectoderm, both during embyrogenesis and in the imaginal discs (see Fig. S1 in the supplementary material) (Khaliullina et al., 2009). In embryos, Mgl levels are highest in cells that produce pigmented structures such as denticles and mouthhooks. In both embryonic and imaginal epithelia, Mgl is found in an apical membrane compartment, similar to its apical localization in kidney epithelial cells (Christensen and Willnow, 1999; Moestrup and Verroust, 2001). To reduce Mgl levels in developing epithelia, we generated RNA interference constructs directed at different regions of the *mgl* transcript, and targeted their expression to different regions of developing animals using the *GAL4/UAS* system (Brand and Perrimon, 1993). When RNA interference is induced in the developing wing disc, it efficiently depletes Mgl protein (Khaliullina et al., 2009). The resulting adult wings are normally patterned, but the appearance of wing cuticle is defective. The adult wing blade consists predominantly of cuticle secreted by wing epithelial cells, most of which undergo apoptosis and are eliminated from the wing shortly after emergence (Johnson and Milner, 1987; Kimura et al., 2004). The cuticle of control wings was transparent and iridescent (Fig. 2A). However, the cuticle synthesized by cells expressing *mgl* RNAi constructs was dull and opaque (Fig. 2B). When *mgl* RNAi was targeted to the posterior compartment, flies emerged with intact wings. However, after several days the posterior wing blade was frayed and broken, suggesting that cuticle secreted by cells missing Mgl is more fragile than cuticle secreted by control cells (Fig. 2C,D). Finally, *mgl* knockdown subtly changed the color of cuticle secreted by wing epithelial cells. In the anterior compartment, where Mgl levels were normal, veins and hairs were brownish in color. In the posterior compartment, where Mgl levels were reduced, they appeared less brown and more black (compare Fig. 2C,E). Thus, Mgl is required to produce cuticle with normal transparency, mechanical resilience and color.

To investigate the basis of these altered cuticle properties, we used electron microscopy to study the different stages of cuticle secretion in control and *mgl* RNAi tissue. We induced *mgl* RNAi in the dorsal compartment of the developing wing, fixed pupal wings at various times and processed them for electron microscopy. We compared the appearance of the dorsal wing blade, both with the ventral region of the same wing, and with dorsal regions from control wings. Knockdown of *mgl* did not perturb formation of the outer envelope or epicuticle (compare Fig. 2G,H). Later, the chitinous procuticle was secreted and its thickness did not differ obviously in *mgl* knockdown tissue. However, the distal procuticle produced by cells with reduced Mgl developed electron-lucent fissures (compare Fig. 2I,J). These became more severe and numerous with time and the procuticle of adult wings was dramatically cracked and split. Despite this, the striated appearance of the procuticle, which reflects the organization of chitin fibers, did not appear to be dramatically disrupted by loss of *mgl* (compare Fig. 2K,L). The tendency of cuticle to form cracks in the procuticle layer probably explains the fragility and opacity of cuticle produced by cells missing Mgl.

Because loss of *mgl* influences both pigmentation and the structural integrity of the cuticle, we wondered whether dopamine levels might be altered. We therefore compared levels of dopamine in control and *mgl* RNAi pupal wings at the time that pigmentation occurs. Directly blocking dopamine synthesis by knockdown of tyrosine hydroxylase strongly reduced dopamine levels in the wing; however, loss of *mgl* did not (see Fig. S2 in the supplementary material).

Wing cuticle pigmentation and stiffness depend on Laccase 2

To further investigate the basis of pigmentation changes caused by loss of *mgl*, we utilized an in vitro melanization assay (Walter et al., 1996). Components required for melanin synthesis are deposited into the cuticle before dopamine is released (Walter et

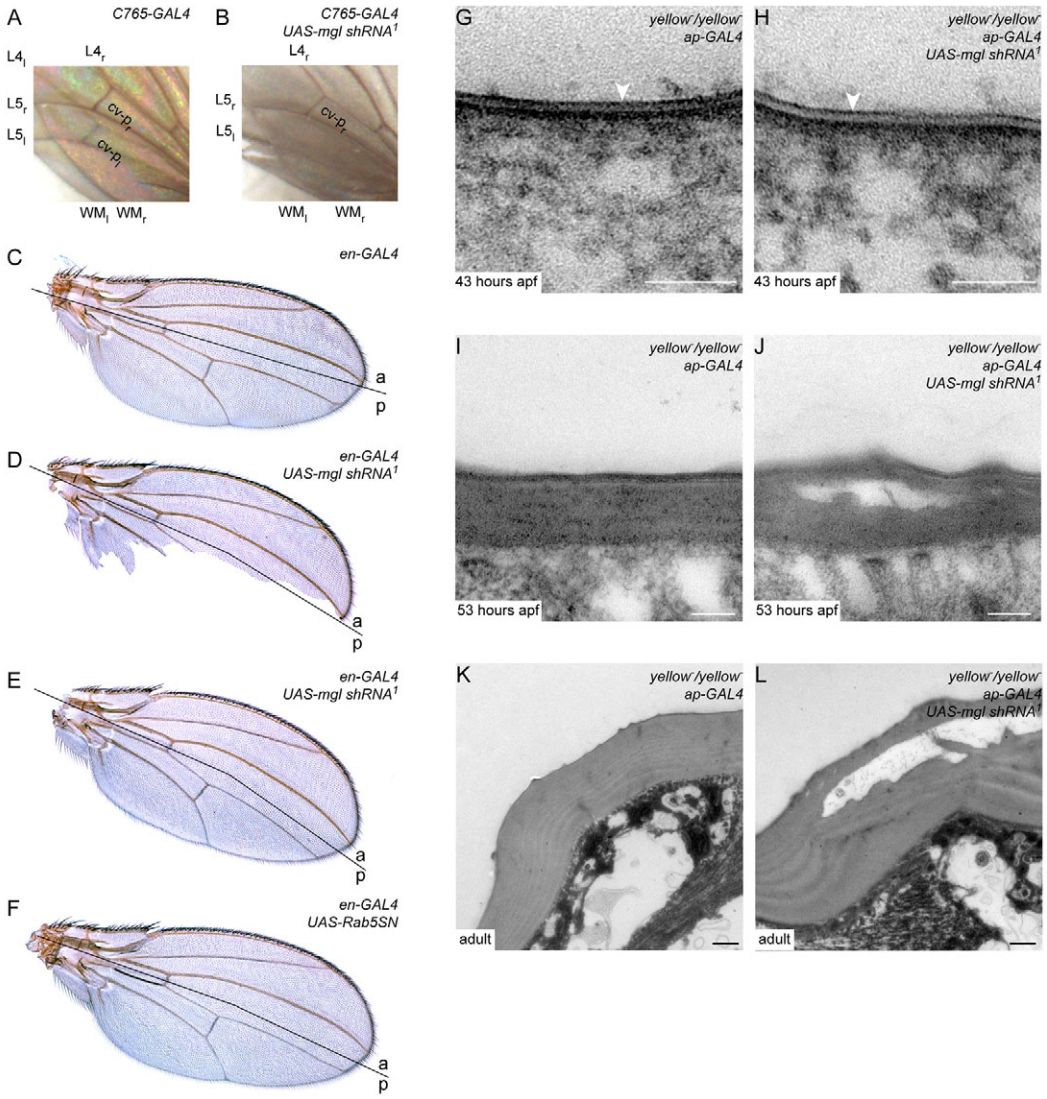

Fig. 2. *Mgl* RNAi perturbs pigmentation and structural integrity of the cuticle. (**A**,**B**) Light micrograph of adult wings from a control living fly (A) and a living fly in which *mgl* RNAi has been induced throughout the wing blade (B). In A, the left wing can be seen underneath the right wing because wings are transparent. The *mgl* RNAi wings shown in B are not transparent, and the left wing cannot be seen underlying the right wing. L4, L5: longitudinal veins 4 and 5, respectively. Subscripts r and l indicate features on right and left wings, respectively. WM, wing margin. (**C-F**) Light micrograph of an adult control wing (C) a wing expressing a *mgl* RNAi construct (D,E) or Rab5SN (F) in the posterior compartment. *Mgl* RNAi causes wing fragility (D). Both *mgl* RNAi and Rab5SN change cuticle pigmentation from brown to grey (E,F). A black line indicates the anteroposterior compartment boundary. (**G-L**) Electron micrograph of the dorsal cuticle of control wings (G,I,K) and wings expressing *mgl* RNAi in the dorsal compartment (H,J,L). All wings are additionally mutant for *yellow.* (G,H) Pupal wings at 43 hours apf (29°C). *Mgl* RNAi (H) does not affect formation of the envelope layer (white arrowheads). (I,J) Pupal wings at 53 hours apf (29°C). *Mgl* RNAi (J) causes fissures in the distal procuticle but does not affect cuticle thickness. (K,L) Adult wings before expansion. *Mgl* RNAi (L) procuticle is split but still exhibits chitin-dependent striations. Scale bars: 80 nm in G,H; 200 nm in I,J; 500 nm in K,L.

al., 1996). When 58-60 hour pupal wings, which had not yet undergone pigmentation, were incubated for 1.5 hours with 5.3 mM dopamine they developed strong pigmentation (Fig. 3A). To confirm that the melanization observed in vitro depends on cuticular enzymes and is not a consequence of auto-oxidation, we tested its dependence on the activity of Laccase 2. Laccase 2 is the phenoloxidase that is required for cuticular tanning in flour beetles (Arakane et al., 2005). RNAi-mediated knockdown of *Drosophila laccase 2* in the posterior compartment of the wing blocked cuticle pigmentation and reduced cuticle stiffness (see Fig. S3A,B in the supplementary material), similar to its function in *Tribolium.* This suggests that Laccase 2 generates both the dopaminoquinone required for melanization, and also quinones derived from N-β-alanyl dopamine or N-acetyl dopamine that participate in sclerotization. When these wings were subjected to in vitro melanization, pigmentation did not develop in the *laccase 2*-deficient posterior compartment (Fig. 3B). Thus, the pigmentation that occurs upon addition of exogenous dopamine to pupal wings reflects in vivo melanin synthesis mechanisms.

To confirm that pigmentation changes caused by *mgl* RNAi in the posterior compartment were not due to differences in dopamine levels, we tested whether provision of exogenous excess dopamine

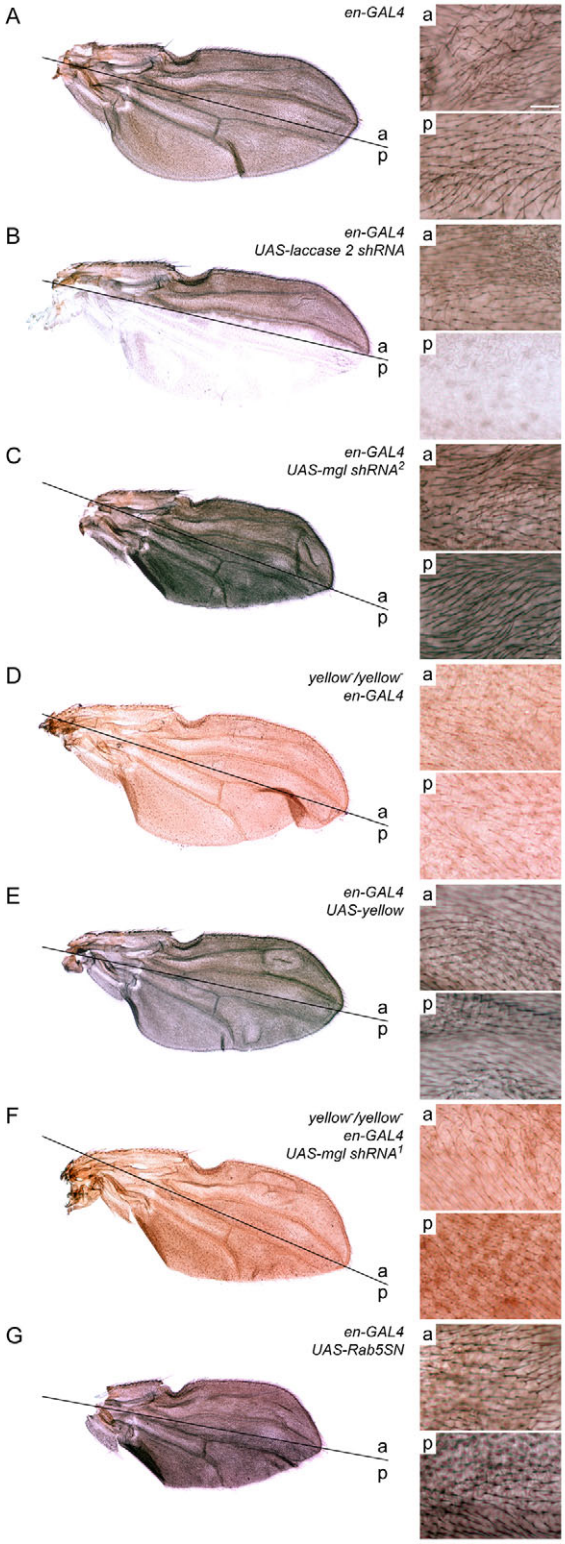

Fig. 3. In vitro melanization is influenced by Mgl, Laccase 2, Yellow and Rab5. (**A-G**) In vitro melanization of pupal wings at 58-60 hours apf (29°C) from animals expressing different constructs in the posterior compartment under control of *en-GAL4*. (A) *en-GAL4* alone, (B) *en-GAL4; UAS-laccase 2 shRNA*, (C) *en-GAL4; pFRIPE-UAS-mgl shRNA*^{2}, (D) *yellow*$^{-}$*/yellow*$^{-}$*; en-GAL4*, (E) *en-GAL4; UAS-yellow*, (F) *yellow*$^{-}$*/yellow*$^{-}$*; en-GAL4; pFRIPE-UAS-mgl shRNA*^{1} and (G) *en-GAL4; pUhr-UAS-Rab5SN*. Left panels show whole wings. Right panels show enlarged regions of the anterior and posterior compartments. A black line indicates the anteroposterior (ap) compartment boundary. Loss of Mgl shifts hair color away from brown and towards black in otherwise wild-type wings (C) but does not do so in *yellow* mutant wings (F). Loss of Mgl also increases the density of wing hairs [compare anterior and posterior compartments in (C,F)]. Increased hair density is a consequence of failure of wing epithelial cells to expand their apical cross section late in pupal development (not shown). This accounts for the denser coloration produced by *mgl* RNAi tissue in the posterior compartment of *yellow* mutant wings. However pigmentation does not change from brown to black. Scale bar: 200 μm.

would equalize the color in the two compartments. Upon incubation with dopamine, the color that develops in the posterior compartment is blacker than that in the anterior. Because in vitro melanized pupal wings develop especially strong pigmentation, this color difference is now obvious, not just in veins, but throughout the wing blade in wing hairs (Fig. 3C). This confirms that the color changes produced by loss of *mgl* are not caused by altered dopamine levels.

Mgl controls cuticle pigmentation by reducing Yellow protein levels

The Yellow protein is required for synthesis of black melanin from dopamine. Addition of excess dopamine to *yellow* mutant pupal wings produced yellowish brown rather than black pigmentation (Fig. 3D). Therefore, we wondered whether the blackish hue resulting from *mgl* knockdown might be caused by increased or ectopically localized Yellow activity. Overexpression of *yellow* did not significantly change the color of the adult wing cuticle (see Fig. S3C in the supplementary material). However, surprisingly, it did change the color produced in the in vitro melanization reaction. *Yellow* overexpression produced the same effect as loss of *mgl* – shifting coloration from brown to black (Fig. 3E). To ask whether Yellow was required for the development of black pigment in *mgl* RNAi tissue, we induced *mgl* RNAi in the posterior compartment of *yellow* mutant wings and subjected them to in vitro melanization. In the *yellow* mutant background, loss of *mgl* no longer changed pigmentation in the posterior compartment (Fig. 3F). This suggests that the changed pigmentation in *mgl* RNAi tissue is caused by excess Yellow activity and that Mgl normally shifts cuticle pigmentation towards brown and away from black by reducing Yellow activity.

We wondered whether excess Yellow activity might also cause the cuticle fissures that develop upon *mgl* knockdown. However, if this were so, then the cuticle defects in *mgl* knockdown tissue should be reversed by removing *yellow*. This was not the case; *mgl* knockdown caused fissures in the distal procuticle in both *yellow*$^{-}$*/yellow*$^{-}$ and *yellow*$^{+}$*/yellow*$^{+}$ wings (see Fig. S4A,B in the supplementary material). Thus, Mgl affects cuticle mechanical properties independently of Yellow. Interestingly, wings missing both Mgl and Yellow curled upwards dramatically after eclosion – a defect never seen in wings missing only one of these proteins (see Fig. S4C-H in the supplementary material). These observations also suggest that Mgl and Yellow contribute independently to cuticle mechanical properties.

To further investigate how Mgl might influence Yellow activity to control pigmentation, we compared Yellow distribution in wild-type and *mgl* RNAi during cuticle formation. Staining with a fluorescent chitin-binding protein showed that procuticle synthesis was underway in control pupae by 60 hours apf (29°C). The emerging procuticle covered the entire apical surface of wing epithelial cells, both over wing hairs and the rest of the apical

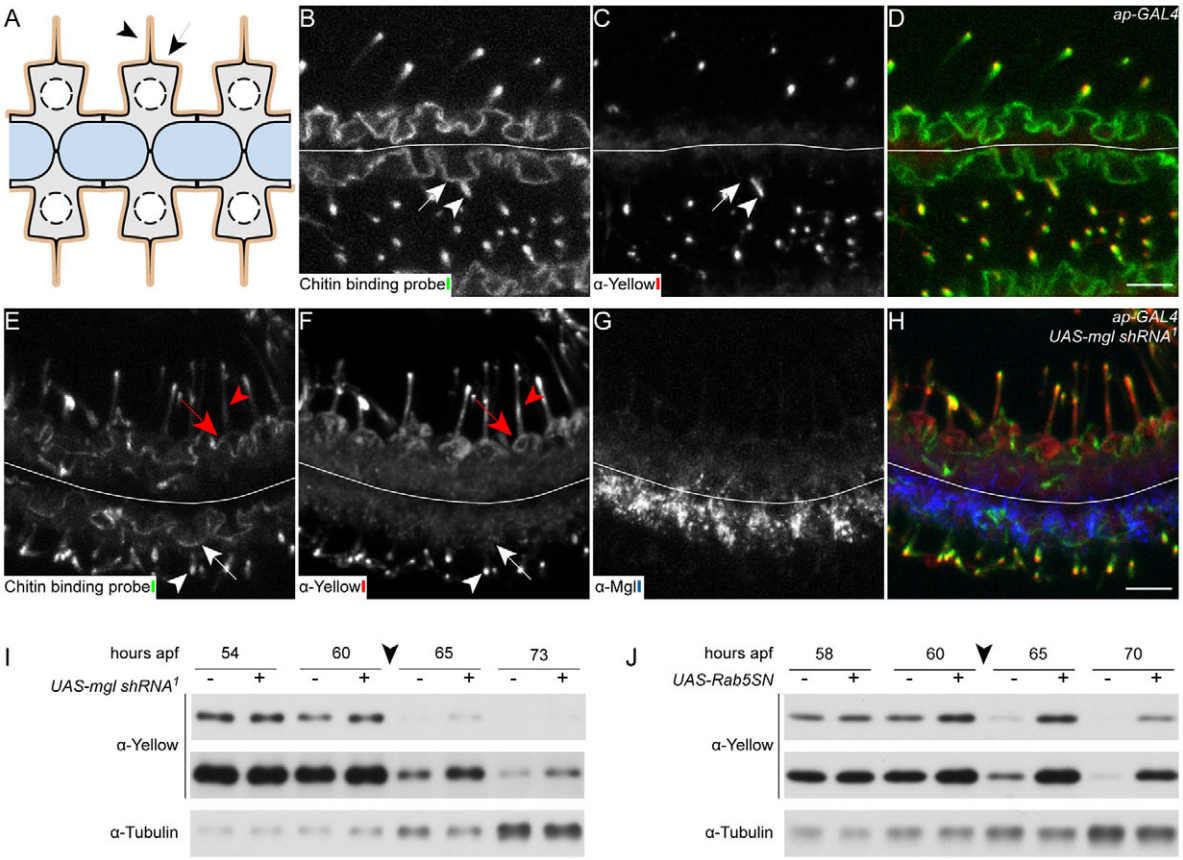

Fig. 4. Mgl RNAi and Rab5SN cause excess accumulation of Yellow. (**A**) Cartoon showing the epithelial organization of the pupal wing at about 60 hours apf (29°C). The dorsal layer is up. Brown, cuticle; gray, cell; white, nucleus; blue, hemolymph/basal extracellular matrix, black solid line: plasma membrane, black interrupted line: nuclear envelope. The arrowhead points at a hair, the arrow at the hair pedestal. (**B-D**) Frozen thin sections of a control wing aged 60 hours apf (29°C) stained for Yellow (C and D red). Cuticle is labeled by a fluorescent chitin-binding probe (B and D green). In contrast to the chitin-binding probe, which gives a signal along the whole apical surface (B,D), Yellow is found specifically in the hairs. Hairs curve out of the plane of the section and often appear in cross section without an obvious connection to the rest of the apical cuticle. (**E-H**) Frozen thin sections of 60 hours apf (29°C) pupal wings in which *mgl* RNAi was induced in the dorsal compartment (top). Wings are stained for chitin (E,H green), Yellow (F,H red) and Mgl (G,H blue). In (B-H), white lines indicate the boundary between the dorsal (top) and ventral compartment. Scale bar in (B-H): 5 μm. Arrowheads point at hairs, arrows at regions between the hairs. (**I**,**J**) Western blots of pupal wings from control (–) flies, or flies expressing either *pFRIPE-UAS-mgl shRNA1* (+ in I) or *pUhr-UAS-Rab5SN* (+ in J) in the dorsal compartment and probed with anti-Yellow or anti-Tubulin. Two different exposures of the anti-Yellow blot are shown. Tubulin levels increase at 65 hours apf (29°C) coincident with the appearance of transalar microtubule arrays (Mogensen and Tucker, 1987), but can be used as an internal standard for similarly aged samples. The procuticle is partially secreted at 54 hours apf (29°C) and completed at 63 hours apf (29°C). Pigmentation begins between 60 and 65 hours apf (29°C) (indicated by arrowhead).

surface. Yellow protein was found specifically in wing hairs, but not in other regions of the apical cuticle, on both the dorsal and ventral wing surfaces (Fig. 4A-D and see Fig. S5A-C in the supplementary material). To ask how Mgl influenced the distribution of Yellow, we induced RNAi against *mgl* in the dorsal compartment. In *mgl* RNAi tissue, Yellow levels were increased in wing hairs and the protein extended into more proximal regions of wing hairs. Yellow also accumulates ectopically in apical regions outside of the hairs (Fig. 4E,F,H). Thus, Mgl is required to reduce Yellow levels and prevent Yellow from accumulating outside of wing hairs.

To ask how Mgl affected total Yellow protein levels, we used western blotting to follow changes in amounts of Yellow protein during cuticle formation and pigmentation. Yellow synthesis begins around the time of cuticle secretion (Mitchell et al., 1983; Walter et al., 1991). In our hands, procuticle was partially formed at 54 hours apf (29°C) and reached its final thickness by 63 hours apf (29°C) (Fig. 2 and not shown). Interestingly, Yellow levels in control wings began to drop before synthesis of the procuticle was complete and were dramatically reduced just before pigmentation began [between 60 and 65 hours apf (29°C)] (Fig. 4I). In *mgl* RNAi wings, Yellow protein levels were initially normal but did not drop as much as in control wings (Fig. 4I). These data suggest that a large fraction of the Yellow protein produced by wing epithelial cells is normally degraded, and that the removal of Yellow requires Mgl. Thus, Mgl is required to ensure both the correct temporal and spatial regulation of Yellow protein levels during cuticle formation.

Mgl promotes Yellow endocytosis

In vertebrates, Mgl internalizes a wide variety of ligands (Christensen and Willnow, 1999; Moestrup and Verroust, 2001). To test whether Mgl might reduce Yellow protein levels via endocytosis, we investigated how Mgl affected Yellow trafficking. Because the

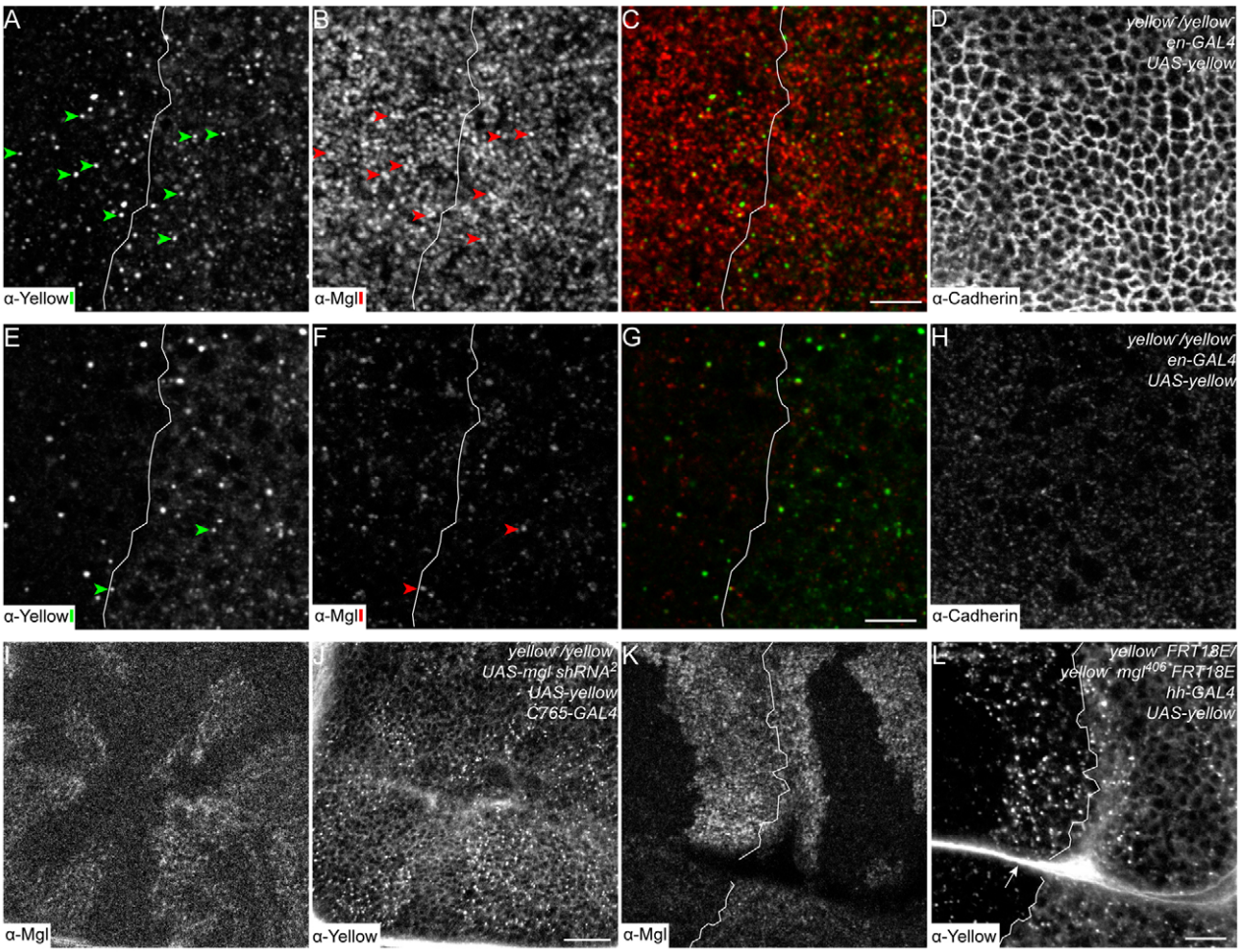

Fig. 5. Loss of *mgl* blocks Yellow endocytosis. (**A-H**) Optical sections of the subapical (A-D) and basolateral (E-H) regions of a third instar wing disc expressing *yellow* in the posterior compartment under the control of *en-GAL4*. Discs are stained for Yellow (A,E and C,G green), Mgl (B,F and C,G red) and Cadherin (D,H). White lines indicate the anteroposterior compartment boundary (posterior cells on the right express *yellow*). Arrowheads indicate colocalization between Yellow and Mgl. (**I**,**J**) Basolateral optical section of a *yellow* mutant wing disc uniformly overexpressing *yellow*, and harboring clones in which *mgl* RNAi has been induced under the control of the GAL4:UAS system (see Materials and methods), stained for Mgl (I) and Yellow (J). Clones are marked by loss of *mgl*. (**K**,**L**) Apical (K) or basolateral (L) optical section of a *yellow* mutant wing disc overexpressing *yellow* in the posterior compartment, and containing *mgl* mutant clones, stained for Mgl (K) and Yellow (L). White line indicates the anteroposterior compartment boundary (posterior cells on the right express *yellow*). The arrow shows where the section crosses the apical lumen that is present in the fold between the wing pouch and the wing, and which contains Yellow. Scale bars: 5 μm in C,G; 20 μm in J; 10 μm in L.

resolution in pupal wing sections was insufficient to study endocytosis, we developed a system to study Yellow trafficking in the third instar wing disc. Yellow is not normally present at this time (Walter et al., 1991); however, when its expression was induced in the posterior compartment using the *GAL4/UAS* system, Yellow was secreted into the apical disc lumen (Fig. 5L, arrow). Although the activity of Yellow is normally cell autonomous when secreted into the cuticle at pupal stages, Yellow protein made by third instar wing discs was not trapped in cuticle and spread from its site of production. Yellow could be observed in punctate structures within cells of the neighboring anterior compartment (Fig. 5A,C, green), suggesting that Yellow is internalized from the apical side of wing disc epithelial cells. A subset of internalized Yellow colocalized with Mgl in apical endosomes (Fig. 5A-C), suggesting that Mgl may internalize Yellow.

To ask whether apical Yellow internalization depended on Mgl, we expressed Yellow throughout the wing disc, and simultaneously induced *mgl* RNAi in clones of cells. In cells missing Mgl, the diffuse Yellow staining was unchanged, but punctate staining disappeared (Fig. 5I,J), suggesting that these cells do not internalize Yellow when Mgl levels are reduced. Internalization of Hedgehog, Wingless and Lipophorin are unaffected by *mgl* RNAi (Khaliullina et al., 2009) (data not shown), suggesting that Mgl is not generally required for internalization in wing discs, but has relatively specific effects on Yellow.

To further investigate the role of Mgl in Yellow endocytosis, and to eliminate the possibility of RNAi off-target effects, we generated *mgl* mutants (Materials and methods; see Fig. S6 in the supplementary material). These mutants were homozygous lethal and died during larval stages, but could be used to produce viable $mgl^{-/-}$ clones of cells within the wing disc. Because $mgl^{-/-}$ clones can be generated independently of the *GAL4/UAS* system, we could visualize their phenotype outside of the region expressing *yellow*. We expressed *yellow* in the posterior compartment under the control of *hh-GAL4*, and generated *mgl* mutant clones throughout the disc. Yellow did not accumulate within non-

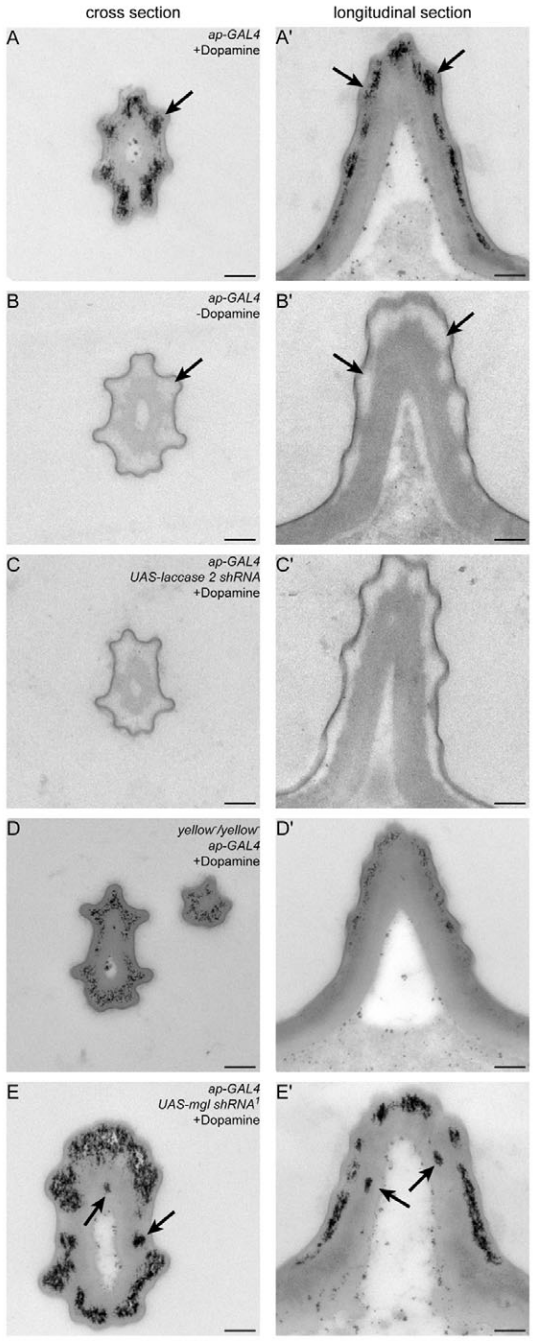

Fig. 6. Restriction of melanin granule formation to the distal procuticle depends on Mgl. (**A-E′**) Electron micrographs of hairs on the dorsal surface of in vitro melanized pupal wings between 59 and 60 hours apf (29°C). Hairs have been sectioned perpendicular to (A-E) or parallel to (A′-E′) the long axis of the hair. All samples have been incubated with dopamine except those in the negative control shown in (B,B′), which have been mock-treated. (A,A′,B,B′) show dorsal hairs from wings of wild-type pupae harboring only the *ap-GAL4* driver. (C,C′) Dorsal hairs from wings of *ap-GAL4; UAS-laccase 2 shRNA* pupae, in which Laccase 2 activity is knocked down on the dorsal side of the wing. (D,D′) Dorsal hairs from wings of *yellow⁻/yellow⁻; ap-GAL4* pupae, which are missing Yellow. (E,E′) Dorsal hairs from wings of *ap-GAL4; pFRIPE-UAS-mgl shRNA1* in which Mgl is knocked down throughout the entire dorsal wing epithelium. Arrows in (A,A′) indicate melanin granules. Arrows in (B,B′) indicate electron lucent regions. Arrows in (E,E′) indicate ectopic melanin granules in proximal regions of the procuticle caused by *mgl* RNAi. Scale bars: 200 nm (A-E′).

expressing cells in *mgl* mutant clones (Fig. 5K,L), confirming that Yellow internalization requires Mgl. Similar loss of Yellow uptake in *mgl* mutant clones was observed in the haltere and leg discs (not shown). These data suggest that Mgl may reduce Yellow protein levels in the pupal wing by promoting its internalization.

To confirm that the reduction in Yellow protein levels and activity depended on endocytosis, we blocked endocytosis starting at the onset of cuticle formation by expressing a dominant negative version of Rab5 (Rab5SN) (Marois et al., 2006). Blocking endocytosis, like loss of *mgl*, delayed the reduction in Yellow protein levels detected by western blotting (Fig. 4I,J). In in vitro melanization assays, regions of wing cuticle synthesized by Rab5SN-expressing cells developed blacker pigmentation, similar to that observed in *mgl* RNAi wings (compare Fig. 3C,G). Finally Rab5SN expression and *mgl* RNAi caused similar pigmentation changes in adult wings (compare Fig. 2E,F). Taken together, these observations indicate that Yellow activity in the cuticle is limited by Mgl- and Rab5-dependent endocytosis.

Mgl-dependent downregulation of Yellow restricts pigmentation to the distal procuticle of wing hairs

To explore whether Mgl-dependent Yellow endocytosis influenced the localization of melanin synthesis within the cuticle, we studied the spatial regulation of melanin production using in vitro melanization and electron microscopy. To unambiguously identify melanin granules, we added exogenous dopamine to pupal wings shortly before the onset of endogenous pigmentation, and looked for electron-dense material, the formation of which depended both on dopamine addition, and on the presence of Laccase 2. In control wings, electron-dense granules formed within a specific layer of the distal procuticle of wing hairs specifically upon addition of dopamine (Fig. 6, compare regions indicated by arrows in A,A′ and B,B′). These granules did not form in the absence of Laccase 2 (Fig. 6C,C′), confirming that they correspond to melanin. In the absence of dopamine addition, this region of the distal procuticle corresponds to a structurally distinct electron lucent layer (arrows in Fig. 6B,B′). This electron lucent layer was absent from the procuticle overlying other apical regions of wing epithelial cells, such as the hair pedestal (see Fig. S5E,F in the supplementary material), and no electron dense granules formed in these regions upon addition of dopamine (see Fig. S5D in the supplementary material). These observations suggest that components required for melanin synthesis are deposited into a specific electron lucent layer of the distal procuticle of wing hairs before pigmentation. Upon release of dopamine by wing epithelial cells, or addition of exogenous dopamine, ultrastructurally observable melanin was produced specifically in this layer.

The restriction of melanin granule formation to wing hairs coincided with the specific localization of Yellow protein to wing hairs by 60 hours apf (29°C) (Fig. 4C). To ask whether formation of ultrastructurally observable melanin granules depended on Yellow, we examined in vitro melanized *yellow* mutant wings in the electron microscope. Granule formation was strongly reduced in *yellow* null mutant wings (compare Fig. 6A,A′ with 6D,D′), suggesting that these granules consist predominantly of Yellow-dependent black melanin.

In *mgl* RNAi tissue, Yellow accumulated to abnormally high levels in wing hairs, and ectopically outside of wing hairs. How is spatial positioning of melanization affected by the failure to efficiently clear excess Yellow protein? Cuticle made by cells missing Mgl did not show ectopic melanization in regions outside

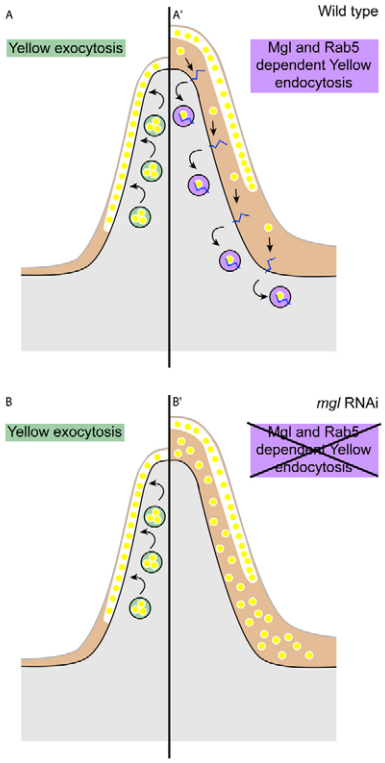

Fig. 7. Model for the function of Mgl in pigmentation. (**A-B′**) Hairs from wild type (A,A′) and *mgl* RNAi (B,B′) pupal wings are depicted. The left (A,B) and right (A′,B′) halves of each picture correspond to different stages of procuticle formation. In A and B, Yellow protein (yellow circles) is being secreted into the distal procuticle, along with other components of the melanin synthesis machinery (white region). Exocytic vesicles are shown in green. Later, in (A′) and (B′), distal procuticle secretion has finished and proximal procuticle secretion is ongoing. After Yellow synthesis stops, Mgl clears Yellow, along with other components of the melanin synthesis machinery, from the extracellular space of wild-type wing cells (A′) (blue lines indicate Mgl and pink indicates endocytic vesicles). In *mgl* RNAi wings (B′), Yellow protein is not downregulated, and the melanin synthesis machinery contaminates the proximal procuticle.

of wing hairs, suggesting that the presence of Yellow alone is insufficient to induce melanization. However, loss of Mgl did cause ectopic formation of melanin granules in wing hair cuticle. Here, melanin granules were no longer restricted to a narrow layer within the distal procuticle but were also found in smaller inclusions in more proximal regions of the procuticle nearer to the assembly zone (Fig. 6E,E′). Thus, Mgl activity is required to restrict the localization of the Yellow-dependent melanin synthesis machinery to its normal distal position within the procuticle. We suggest that rapid Mgl-dependent clearance of Yellow, and possibly other components of the melanin synthesis machinery, occurs after biosynthesis stops and is necessary to prevent contamination of more proximal cuticle layers with these proteins (Fig. 7).

DISCUSSION

How epidermal cells build a cuticle with a precise spatial organization is a fascinating problem. The observation that proteins present in distal regions of the procuticle are synthesized before those located more proximally has led to the idea that the spatial organization of distinct cuticle layers is a consequence of the temporal regulation of cuticle protein biosynthesis and secretion (Doctor et al., 1985; Fristrom et al., 1986; Wolfgang et al., 1986). Although this is probably an important basis of cuticle structuring, we show that it is not sufficient to explain the precision with which different cuticle layers are segregated. Our studies suggest that endocytic clearance of layer-specific cuticle components is essential for the efficient spatial segregation of cuticle layers. This idea is based on the effects of Mgl knockdown on Yellow trafficking and on the spatial restriction of melanization in the wing. We show that the formation of melanin granules is normally restricted to a narrow region within the distal procuticle of wing hairs, and that melanin formation here depends on Yellow. Yellow protein is synthesized during procuticle secretion, but Mgl- and Rab5-dependent endocytosis rapidly reduces its levels before pigmentation begins. This rapid reduction in Yellow, and possibly other components of the melanization machinery, is necessary to restrict melanization to the distal procuticle. This is consistent with a model in which molecules required for eumelanin synthesis are deposited in wing hairs during secretion of the distal procuticle. Mgl-dependent endocytosis rapidly clears these molecules from the assembly zone once their synthesis has stopped. If components of the melanin synthesis machinery are not promptly resorbed by Mgl, they contaminate more proximal layers as cuticle secretion continues (Fig. 7).

Ultrastructurally observable melanin granules form specifically in wing hair cuticle and not over other regions of the apical surface of the same cell. This narrow restriction raises the possibility that specific delivery pathways directed into wing hairs may support not only hair outgrowth, but secretion of specific components into wing hair cuticle. Yellow protein is normally tightly restricted to wing hairs, but loss of Mgl allows it to spread to other regions. Thus, Mgl-dependent endocytosis may not only restrict proteins to particular cuticle layers, but might also prevent lateral spreading away from their delivery site, allowing tight localization to specific subregions of cuticle made by a single cell.

Whereas this study focuses on how Mgl influences pigmentation via trafficking of Yellow, Mgl probably regulates cuticle development by additional mechanisms. The effects of Mgl on the structural integrity of the cuticle in unpigmented regions appears to be independent of Yellow. Furthermore, we observe that loss of Mgl suppresses the formation of excess black melanin in *ebony* mutant wings (F.R. and S.E., unpublished observation). This is unlikely to be a consequence of abnormally high levels of Yellow, because Yellow promotes formation of black melanin. Thus, Mgl-dependent endocytosis may have multiple roles in regulating cuticle assembly. Megalin internalizes a huge variety of different substances in vertebrate tissues, and we speculate that it may have similarly general and pleiotropic functions in restricting the accumulation of different constituents of the cuticle.

Acknowledgements

We thank K. Simons, E. Knust and J. Verbavatz for critical comments on the manuscript. We thank A. Hall for help in generating *mgl* mutants, A. Mahmoud and E. Marois for generating *mgl* RNAi constructs, and C. Böckel for genetics advice. We are grateful to M. Wilsch-Bräuniger for help with electron microscopy. A. Kumichel and N. Muschalik provided help with frozen sections. We thank S. Carroll for the anti-Yellow antibody and *UAS-yellow* flies, and E. Knust for the anti-Crumbs antibody. This work was supported by a grant from the Deutsche Forschungsgemeinschaft to S.E. and by the Max Planck Gesellschaft.

Competing interests statement

The authors declare no competing financial interests.

Supplementary material

Supplementary material for this article is available at
http://dev.biologists.org/lookup/suppl/doi:10.1242/dev.056309/-/DC1

References

Andersen, S. O. (2009). Insect cuticular sclerotization: a review. *Insect Biochem. Mol. Biol.* **40**, 166-178.

Arakane, Y., Muthukrishnan, S., Beeman, R. W., Kanost, M. R. and Kramer, K. J. (2005). Laccase 2 is the phenoloxidase gene required for beetle cuticle tanning. *Proc. Natl. Acad. Sci. USA* **102**, 11337-11342.

Brand, A. H. and Perrimon, N. (1993). Targeted gene expression as a means of altering cell fates and generating dominant phenotypes. *Development* **118**, 401-415.

Christensen, E. I. and Willnow, T. E. (1999). Essential role of megalin in renal proximal tubule for vitamin homeostasis. *J. Am. Soc. Nephrol.* **10**, 2224-2236.

Devine, W. P., Lubarsky, B., Shaw, K., Luschnig, S., Messina, L. and Krasnow, M. A. (2005). Requirement for chitin biosynthesis in epithelial tube morphogenesis. *Proc. Natl. Acad. Sci. USA* **102**, 17014-17019.

Dietzl, G., Chen, D., Schnorrer, F., Su, K. C., Barinova, Y., Fellner, M., Gasser, B., Kinsey, K., Oppel, S., Scheiblauer, S. et al. (2007). A genome-wide transgenic RNAi library for conditional gene inactivation in Drosophila. *Nature* **448**, 151-156.

Doctor, J., Fristrom, D. and Fristrom, J. W. (1985). The pupal cuticle of Drosophila: biphasic synthesis of pupal cuticle proteins in vivo and in vitro in response to 20-hydroxyecdysone. *J. Cell Biol.* **101**, 189-200.

Fristrom, J. W., Alexander, S., Brown, E., Doctor, J., Fechtel, K., Fristrom, D., Kimbrell, D., King, D. and Wolfgang, W. J. (1986). Ecdysone regulation of cuticle protein gene expression in Drosophila. *Arch. Insect Biochem. Physiol.* **3**, 119-132.

Han, Q., Fang, J., Ding, H., Johnson, J. K., Christensen, B. M. and Li, J. (2002). Identification of Drosophila melanogaster yellow-f and yellow-f2 proteins as dopachrome-conversion enzymes. *Biochem. J.* **368**, 333-340.

Hong, S. T., Bang, S., Paik, D., Kang, J., Hwang, S., Jeon, K., Chun, B., Hyun, S., Lee, Y. and Kim, J. (2006). Histamine and its receptors modulate temperature-preference behaviors in Drosophila. *J. Neurosci.* **26**, 7245-7256.

Hopkins, T. L. and Kramer, K. J. (1992). Insect cuticle sclerotization. *Annu. Rev. Entomol.* **37**, 273-302.

Johnson, S. A. and Milner, M. J. (1987). The final stages of wing development in Drosophila melanogaster. *Tissue Cell* **19**, 505-513.

Kayser-Wegmann, I. (1976). Differences in black pigmentation in lepidopteran cuticles as revealed by light and electron microscopy. *Cell Tissue Res.* **171**, 513-521.

Khaliullina, H., Panakova, D., Eugster, C., Riedel, F., Carvalho, M. and Eaton, S. (2009). Patched regulates Smoothened trafficking using lipoprotein-derived lipids. *Development* **136**, 4111-4121.

Kimura, K., Kodama, A., Hayasaka, Y. and Ohta, T. (2004). Activation of the cAMP/PKA signaling pathway is required for post-ecdysial cell death in wing epidermal cells of Drosophila melanogaster. *Development* **131**, 1597-1606.

Kornezos, A. and Chia, W. (1992). Apical secretion and association of the Drosophila yellow gene product with developing larval cuticle structures during embryogenesis. *Mol. Gen. Genet.* **235**, 397-405.

Latocha, M., Chodurek, E., Kurkiewicz, S., Swiatkowska, L. and Wilczok, T. (2000). Pyrolytic GC-MS analysis of melanin from black, gray and yellow strains of Drosophila melanogaster. *J. Anal. Appl. Pyrolysis* **56**, 89-98.

Locke, M. (2001). The Wigglesworth Lecture: Insects for studying fundamental problems in biology. *J. Insect Physiol.* **47**, 495-507.

Marois, E. and Eaton, S. (2007). RNAi in the Hedgehog signaling pathway: pFRiPE, a vector for temporally and spatially controlled RNAi in Drosophila. *Methods Mol. Biol.* **397**, 115-128.

Marois, E., Mahmoud, A. and Eaton, S. (2006). The endocytic pathway and formation of the Wingless morphogen gradient. *Development* **133**, 307-317.

Mitchell, H. K., Roach, J. and Petersen, N. S. (1983). The morphogenesis of cell hairs on Drosophila wings. *Dev. Biol.* **95**, 387-398.

Moestrup, S. K. and Verroust, P. J. (2001). Megalin- and cubilin-mediated endocytosis of protein-bound vitamins, lipids, and hormones in polarized epithelia. *Annu. Rev. Nutr.* **21**, 407-428.

Mogensen, M. M. and Tucker, J. B. (1987). Evidence for microtubule nucleation at plasma membrane-associated sites in Drosophila. *J. Cell Sci.* **88**, 95-107.

Moussian, B. (2010). Recent advances in understanding mechanisms of insect cuticle differentiation. *Insect Biochem. Mol. Biol.* **40**, 363-375.

Moussian, B., Seifarth, C., Müller, U., Berger, J. and Schwarz, H. (2006). Cuticle differentiation during Drosophila embryogenesis. *Arthropod. Struct. Dev.* **35**, 137-152.

Oda, H., Uemura, T., Harada, Y., Iwai, Y. and Takeichi, M. (1994). A Drosophila homolog of cadherin associated with armadillo and essential for embryonic cell-cell adhesion. *Dev. Biol.* **165**, 716-726.

Patel, N. H., Snow, P. M. and Goodman, C. S. (1987). Characterization and cloning of fasciclin III: a glycoprotein expressed on a subset of neurons and axon pathways in Drosophila. *Cell* **48**, 975-988.

Richard, M., Grawe, F. and Knust, E. (2006). DPATJ plays a role in retinal morphogenesis and protects against light-dependent degeneration of photoreceptor cells in the Drosophila eye. *Dev. Dyn.* **235**, 895-907.

Sugumaran, M. (2002). Comparative biochemistry of eumelanogenesis and the protective roles of phenoloxidase and melanin in insects. *Pigment Cell Res.* **15**, 2-9.

True, J. R., Yeh, S. D., Hovemann, B. T., Kemme, T., Meinertzhagen, I. A., Edwards, T. N., Liou, S. R., Han, Q. and Li, J. (2005). Drosophila tan encodes a novel hydrolase required in pigmentation and vision. *PLoS Genet.* **1**, e63.

Vincent, J. F. and Wegst, U. G. (2004). Design and mechanical properties of insect cuticle. *Arthropod. Struct. Dev.* **33**, 187-199.

Walter, M. F., Black, B. C., Afshar, G., Kermabon, A. Y., Wright, T. R. and Biessmann, H. (1991). Temporal and spatial expression of the yellow gene in correlation with cuticle formation and dopa decarboxylase activity in Drosophila development. *Dev. Biol.* **147**, 32-45.

Walter, M. F., Zeineh, L. L., Black, B. C., McIvor, W. E., Wright, T. R. and Biessmann, H. (1996). Catecholamine metabolism and in vitro induction of premature cuticle melanization in wild type and pigmentation mutants of Drosophila melanogaster. *Arch. Insect Biochem. Physiol.* **31**, 219-233.

Wittkopp, P. J. and Beldade, P. (2009). Development and evolution of insect pigmentation: genetic mechanisms and the potential consequences of pleiotropy. *Semin. Cell Dev. Biol.* **20**, 65-71.

Wittkopp, P. J., True, J. R. and Carroll, S. B. (2002). Reciprocal functions of the Drosophila yellow and ebony proteins in the development and evolution of pigment patterns. *Development* **129**, 1849-1858.

Wolfgang, W. J., Fristrom, D. and Fristrom, J. W. (1986). The pupal cuticle of Drosophila: differential ultrastructural immunolocalization of cuticle proteins. *J. Cell Biol.* **102**, 306-311.

Wright, T. R. (1987). The genetics of biogenic amine metabolism, sclerotization, and melanization in Drosophila melanogaster. *Adv. Genet.* **24**, 127-222.

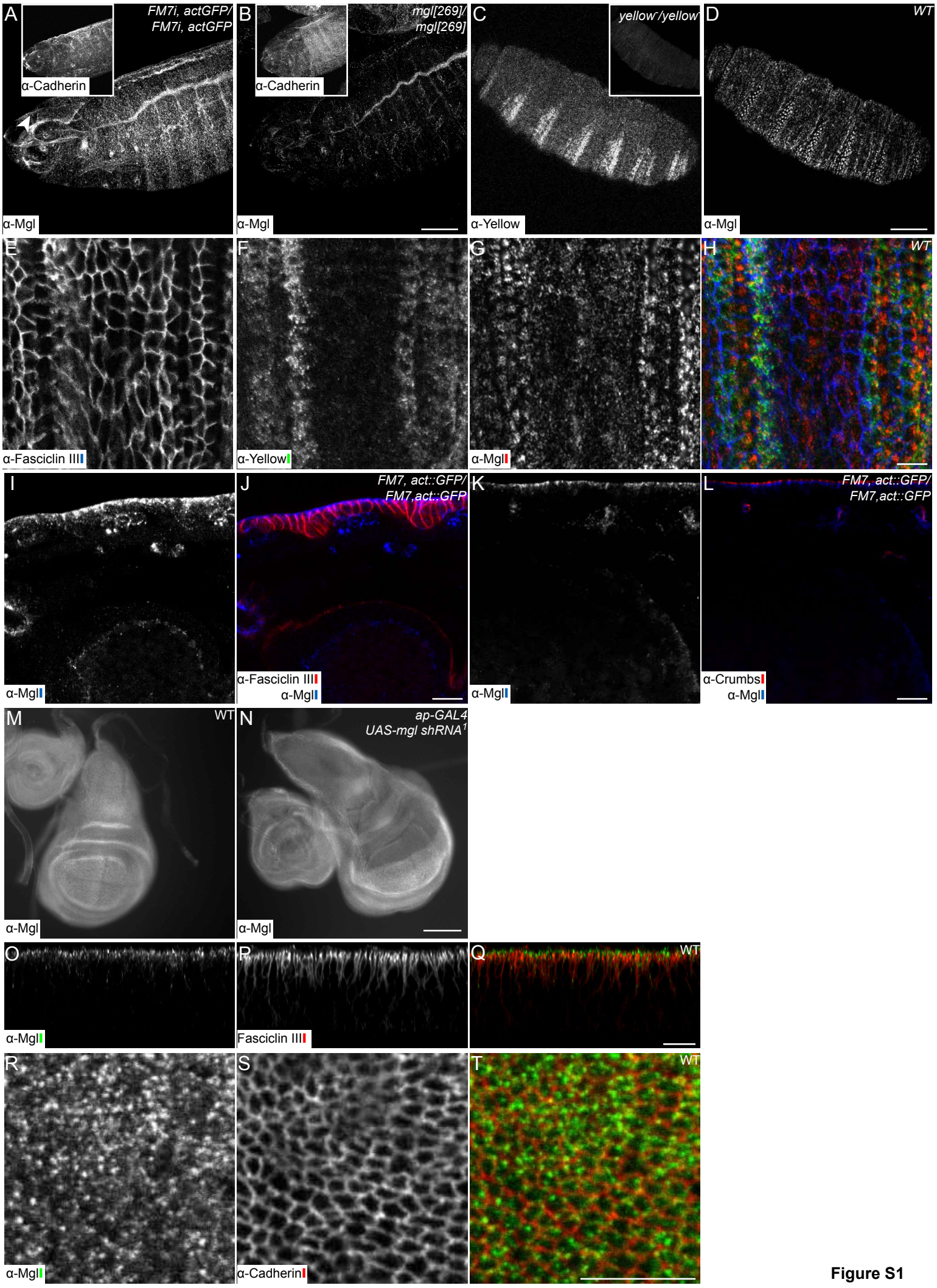
A
FM7i, actGFP/
FM7i, actGFP
α-Cadherin
α-Mgl
B
mgl[269]/
mgl[269]
α-Cadherin
α-Mgl
C
yellow-/yellow-
α-Yellow
D
WT
α-Mgl
E
α-Fasciclin III
F
α-Yellow
G
α-Mgl
H
WT
I
α-Mgl
J
FM7, act::GFP/
FM7,act::GFP
α-Fasciclin III
α-Mgl
K
α-Mgl
L
FM7, act::GFP/
FM7,act::GFP
α-Crumbs
α-Mgl
M
WT
α-Mgl
N
ap-GAL4
UAS-mgl shRNA1
α-Mgl
O
α-Mgl
P
Fasciclin III
Q
WT
R
α-Mgl
S
α-Cadherin
T
WT

Figure S1

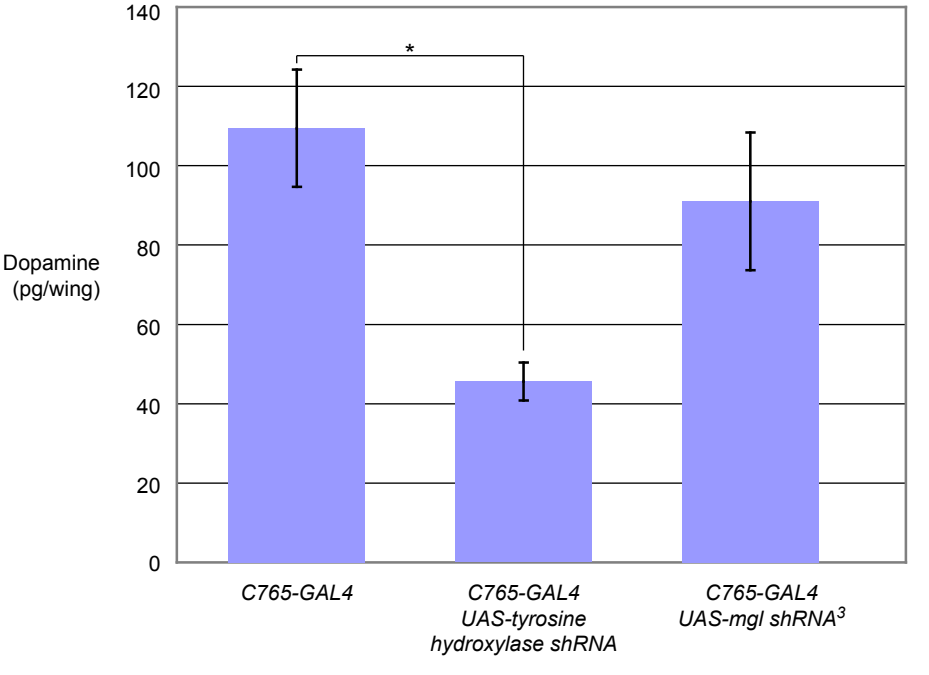
Dopamine
(pg/wing)
140
120
100
80
60
40
20
0
*
C765-GAL4
C765-GAL4
UAS-tyrosine
hydroxylase shRNA
C765-GAL4
UAS-mgl shRNA3

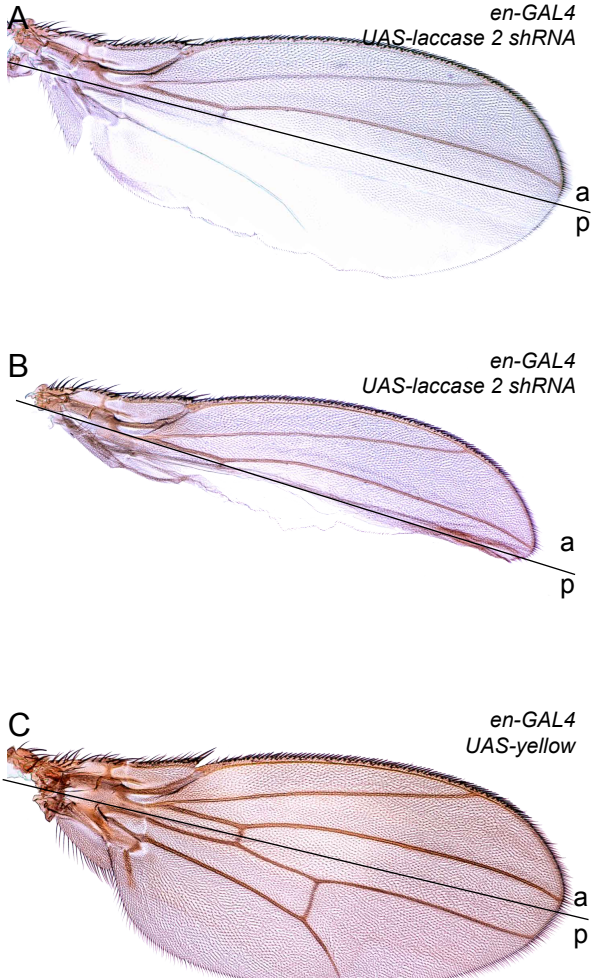
A
en-GAL4
UAS-laccase 2 shRNA
a
p
B
en-GAL4
UAS-laccase 2 shRNA
a
p
C
en-GAL4
UAS-yellow
a
p

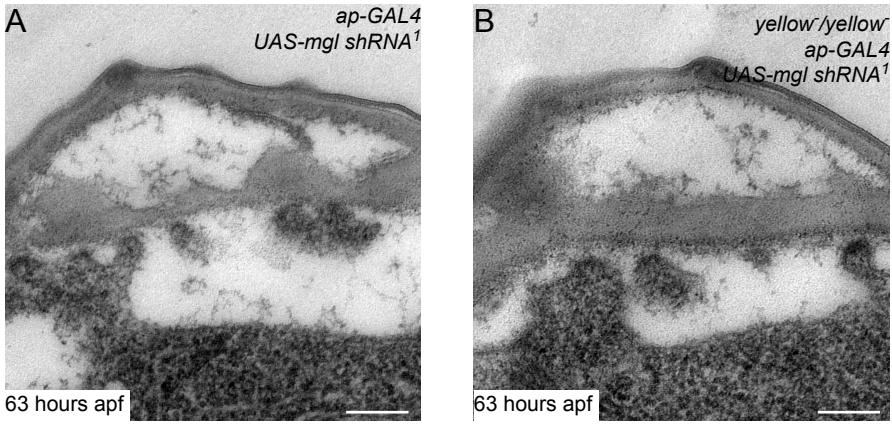
A
ap-GAL4
UAS-mgl shRNA1
63 hours apf
B
yellow-/yellow-
ap-GAL4
UAS-mgl shRNA1
63 hours apf

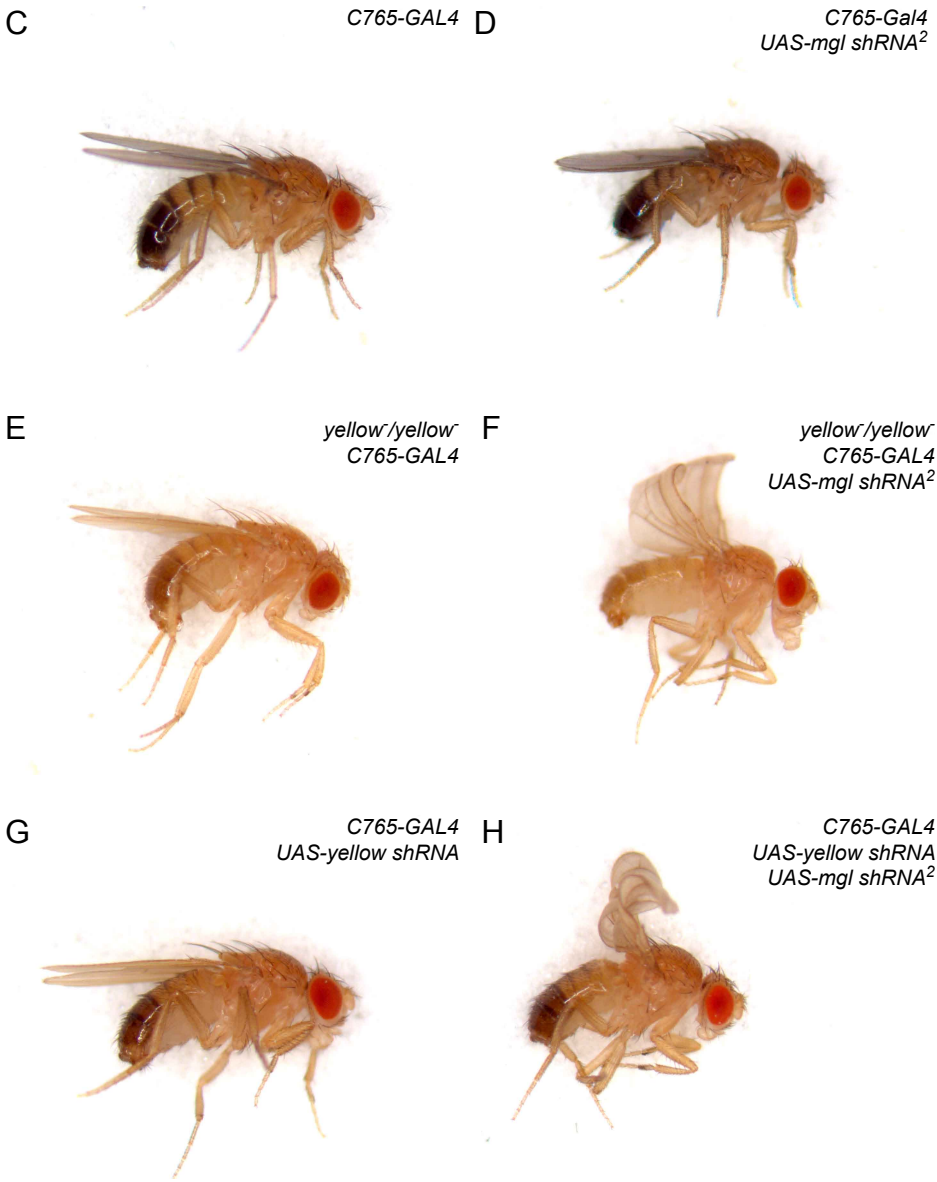
C
C765-GAL4
D
C765-Gal4
UAS-mgl shRNA2
E
yellow-/yellow-
C765-GAL4
F
yellow-/yellow-
C765-GAL4
UAS-mgl shRNA2
G
C765-GAL4
UAS-yellow shRNA
H
C765-GAL4
UAS-yellow shRNA
UAS-mgl shRNA2

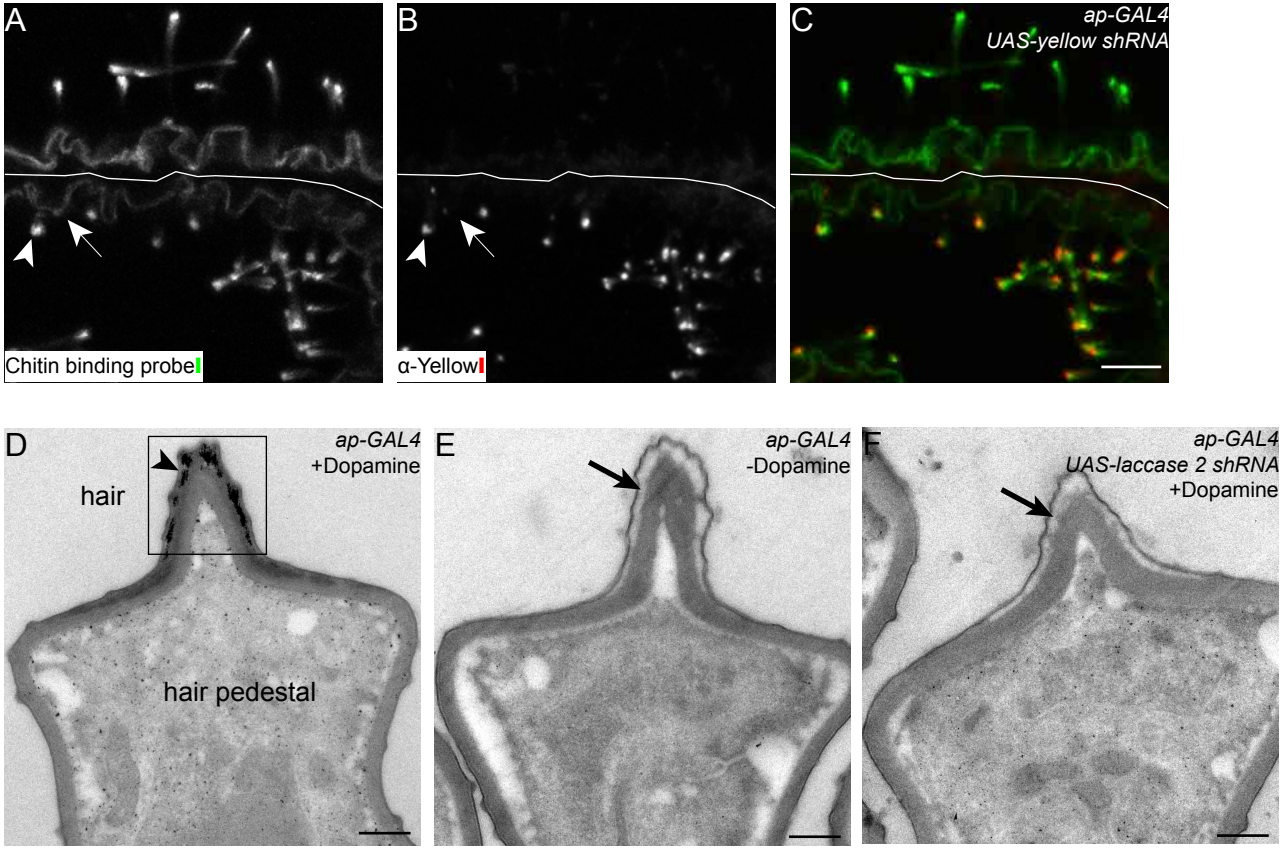
A
Chitin binding probe
B
α-Yellow
C
ap-GAL4
UAS-yellow shRNA
D
hair
hair pedestal
ap-GAL4
+Dopamine
E
ap-GAL4
-Dopamine
F
ap-GAL4
UAS-laccase 2 shRNA
+Dopamine

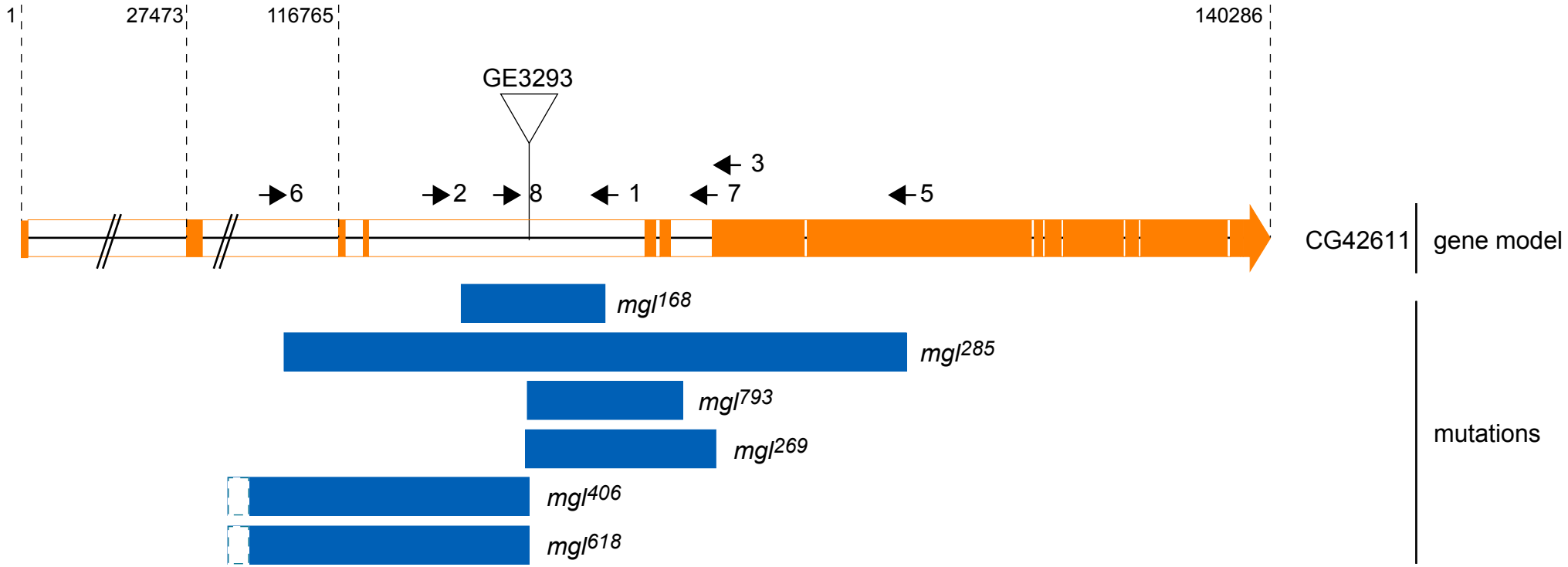

Allele	Deleted nucleotides of CG42611	Viability	Coding sequence	Protein levels*	P-element GE3293	Clones**	Yellow uptake***	PCR to amplify the sequence flanking the deletion****	
								Primer pair (5'-3')	Amplicon
mgl[168]	119875 – 123577	lethal	unaffected	undetectable	excised	not tested	not tested	1: CAGTACTTGTAAAAACTGGG 2: GCACAATAATTTATCGCGCTTA	333 bp
mgl[269]	121585 – 126308	lethal	affected	undetectable	completely present	yes	not tested	3: TTATCGCCCACCCAGTCGAC 4: CGACGGGACCACCTTATG	428 bp
mgl[285]	115520 – 131136	lethal	affected	undetectable	excised	yes	reduced	5: CTGGAAGACTACAATGGGAT 6: AAAAAGGGGTTCCAAAATGG	422 bp
mgl[406]	<39167 - 121585	lethal	affected	undetectable	partially present	yes	reduced	not applicable	
mgl[608]	<39167 - 121585	lethal	affected	undetectable	excised	not tested	not tested	not applicable	
mgl[793]	121585 - 125550	viable	affected	normal	excised	not tested	not tested	7: TGGGTCAGGTAATGCAAATA 8: GTTAACTGTCTCATAAACTG	956 bp